Geophysical Research Letters

RESEARCH LETTER
10.1029/2018GL077537

Clonal Vegetation Patterns Mediate Shoreline Erosion

Brittany M. Bernik[1,2], Maarten B. Eppinga[3], Alexander S. Kolker[4,5], and Michael J. Blum[1,2]

[1]Department of Ecology and Evolutionary Biology, Tulane University, New Orleans, LA, USA, [2]The ByWater Institute, Tulane University, New Orleans, LA, USA, [3]Department of Environmental Science, Copernicus Institute of Sustainable Development, Utrecht University, Utrecht, Netherlands, [4]Louisiana Universities Marine Consortium, Chauvin, LA, USA, [5]Department of Earth and Environmental Sciences, Tulane University, New Orleans, LA, USA

Key Points:
- Analytical and simulation models show the role of biogeomorphic heterogeneity in mediating marsh shoreline erosion under wind wave forces
- Acceleration of marsh erosion is greatest when soil spatial heterogeneity is organized by clonal vegetation patches of intermediate size
- The variability of annual erosion rates and roughness of marsh shorelines increase with the size of clonal vegetation patches

Supporting Information:
- Supporting Information S1
- Data Set S1
- Data Set S2
- Data Set S3

Correspondence to:
M. J. Blum,
mjblum@tulane.edu

Citation:
Bernik, B. M., Eppinga, M. B., Kolker, A. S., & Blum, M. J. (2018). Clonal vegetation patterns mediate shoreline erosion. *Geophysical Research Letters, 45*, 6476–6484. https://doi.org/10.1029/2018GL077537

Received 9 FEB 2018
Accepted 7 JUN 2018
Accepted article online 15 JUN 2018
Published online 5 JUL 2018

Abstract Understanding processes governing coastal erosion is becoming increasingly urgent because highly valued ecosystems like salt marshes are being lost at accelerating rates. Here we examine the role of biotic interactions in mediating marsh shoreline erosion under wind wave forces. We parameterized analytical and cellular automata models with field data to assess how soil heterogeneity among clonal patches of an ecosystem engineer mediates spatiotemporal patterns of marsh shoreline erosion. We found that spatial heterogeneity accelerates erosion, especially when it is organized in patches of intermediate size. Patch size also mediated interannual variability in erosion and strongly controlled shoreline roughness. Our results indicate that shoreline roughness can be diagnostic of internal biological structure and spatiotemporal variability in erosion. Hence, measures of shoreline roughness may inform the timeframe and spatial extent needed to accurately monitor erosion. These findings highlight how the physical response of marsh shorelines to wind wave erosion is a function of landscape ecology.

Plain Language Summary Understanding processes governing coastal erosion is becoming increasingly urgent as highly valued ecosystems like salt marshes are being lost at accelerating rates. This paper investigates how marsh shoreline erosion is affected by the spatial composition of clonal plants. Plant "engineer" species are known to increase soil shear strength, decreasing rates of erosion. Consequently, phenotypic variation among clonal individuals may affect shoreline erosion. Because erosion proceeds as an advancing front, it may be influenced by how soil resistance is spatially organized. We found that, while random variation increased erosion rates, the effect was stronger when variation was organized into clonal patches—particularly ones that were intermediately sized. With increasing clone size, shoreline shape became rougher, and the variability of annual erosion rates increased. Not only does this highlight how a physical process is shaped by biotic attributes, it also shows how the resulting shoreline shape may be diagnostic of biological structure and influence.

1. Introduction

Global loss of highly valued coastal marsh ecosystems has been accelerating due to increasing natural and anthropogenic subsidence, inundation, and erosion (Millennium Ecosystem Assessment, 2005). Understanding how marsh vegetation mediates ecosystem responses to stressors may be key to the success of efforts to stem further loss and to restore coastal marshes (Kirwan & Temmerman, 2009). Mechanistic numerical models have been developed to provide predictive frameworks for understanding processes that maintain marsh elevation in dynamic equilibrium with sea level, including biotic forcings and feedbacks (Fagherazzi et al., 2012, 2013). Substantive progress also has been made toward characterizing lateral marsh loss under wind-wave forces (e.g., Kolker et al., 2011; Leonardi & Fagherazzi, 2014, 2015; Wilson & Allison, 2008), but so far, little consideration has been given to biogeomorphic interactions in models of shoreline erosion (Larsen et al., 2016; but see Mariotti & Fagherazzi, 2010; Möller et al., 2014; Wilson et al., 2012).

Coastal marshes are often dominated by landform engineers that influence soil properties governing erosion resistance (Corenblit et al., 2011). In salt marshes, for example, *Spartina alterniflora* (smooth cordgrass) exhibits functional traits that can influence soil shear strength by contributing to soil organic content and by physically binding the soil matrix (Francalanci et al., 2013; Turner, 2011; van Eerdt, 1985; Zengel et al., 2015). Phenotypic variation in smooth cordgrass can consequently give rise to spatial heterogeneity in soil properties affecting erosion rates (Figures S1 and S2 in the supporting information; see Text S1 and S2 in the supporting information for details; Bernik, 2015). Given the clonal growth form of marsh species like smooth cordgrass, spatial heterogeneity is likely to be nonrandom, corresponding to the distribution of trait

differences among individual clones. Population dynamics and other factors that shape the mosaic composition of clones (e.g., marsh age, where older marshes typically contain larger clonal patches; Travis & Hester, 2005) can also contribute to the spatial organization of heterogeneous landform engineering. Thus, variation in erosion along a marsh shoreline might reflect attributes of constituent plants like smooth cordgrass.

Several other factors suggest that patch-scale biological patterning of marsh heterogeneity can give rise to emergent shoreline erosion dynamics. Recent simulation studies have shown that under low wave power, random spatial heterogeneity can reduce shoreline erosion and increase the roughness of its shape (Leonardi & Fagherazzi, 2014, 2015). Consequently, scaling or averaging local erosion resistances may contribute to the high uncertainty observed in predictive models of marsh erosion (Marani et al., 2011; McLoughlin et al., 2015). Work in materials science also indicates that, not only front propagation processes analogous to shoreline erosion are affected by the range of spatial variation (Kolwankar et al., 2003; Xin, 2000), but also its spatial organization. For example, rates of dissolution can be affected by the patch size of spatial heterogeneities (over a ±40% size range; Štěpánek, 2008). This suggests that variability in clone size (commonly $\pm 4 \times 10^4$%; Travis & Hester, 2005) and identity might explain variation in erosion dynamics. It also raises the possibility that the relative contribution of different factors to erosional processes can be inferred from shoreline patterning (Leonardi, Defne, et al., 2016).

Here we show that marsh shoreline erosion can be strongly influenced by the spatial distribution of biogeomorphic heterogeneity. In this study, we modified and combined existing modeling frameworks to examine whether spatial heterogeneity in soil shear strength attributable to phenotypic variation and clonal organization of smooth cordgrass mediates wind-wave shoreline erosion. The framework presented by Marani et al. (2011) links soil shear strength with marsh erosion rates that can be parameterized from field-derived data, and Leonardi and Fagherazzi (2014, 2015) provide a spatially explicit framework for examining within-site heterogeneity. We integrated the two frameworks and parameterized the resulting model using high resolution data on soil shear strength and shoreline erosion from a Louisiana salt marsh, supplemented with regional measures of wind and wave characteristics. After first illustrating that the modeling approach predicts variation in erosion along a heterogeneous shoreline at the study site, we estimate and compare the effect of clonal organization on average erosion rates and spatiotemporal patterns of erosion under different scenarios of spatial heterogeneity.

2. Methods

2.1. Theory and Model Formulation

We modified the model of Leonardi and Fagherazzi (2014, 2015) by including an alternative formulation for the relationship between inbound wave power and marsh erosion. This involved incorporating a spatially explicit formulation of dimensional relationships between marsh erosion properties proposed by Marani et al. (2011):

$$\frac{Rhc}{\overline{P}} = f\left(\frac{h}{d}\right) \tag{1}$$

where R is erosion rate (in m yr^{-1}), $\overline{P}$ is mean wave power density upon impact (in Wm^{-1}), and $f(\ )$ is a function (dimensionless) relating h, the height of the marsh cliff face above the tidal flat bottom (in m), with d, the depth of the tidal flat bottom with respect to sea level (in m). The parameter c represents soil shear strength (in kPa), which increases through the stabilizing effects of marsh vegetation (Table 1).

For a given site, Marani et al. (2011) showed that $Rh/\overline{P}$ is independent from h/d, so that if constant c is assumed, $f(h/d)/c$ can be considered approximately constant:

$$f(h/d)/c \cong a \tag{2}$$

Substituting equation (2) into equation (1) and solving for the volumetric erosion rate (per unit length) yields the proportionality:

$$R{\cdot}h = a\overline{P} \tag{3}$$

Equation (3) is well supported by empirical observations of erosion rates across marshes (Marani et al., 2011). However, within-site applications are characterized by large unexplained variation (Marani et al., 2011). The

Table 1
Interpretation and Units of the Symbols Used in the Model Formulation

Symbol	Interpretation	Unit (s)
	Marsh erosion as a function of inbound wave power (equations (1)–(5))	
$\overline{P}$	Average wave power density upon impact along a marsh shoreline	W m^{-1}
$\vec{P}$	Wave power density prior to impact	W m^{-1}
$\alpha_{(x,y,t)}$	Angle of $\vec{P}$ relative to the shore-normal at position (x,y) and time t	—
R	Annual erosion rate of a marsh shoreline	m yr^{-1}
c	Soil shear strength along a marsh shoreline	kPa
h	Height of the marsh cliff face above the tidal flat bottom	m
d	Depth of the tidal flat bottom with respect to sea level	m
$f(\frac{h}{d})$	Dimensionless function relating h and d to R	—
φ	Site-specific constant $(f(h/d)/h)$ relating wave power density and soil shear strength to erosion rate (including a conversion from year to s)	m^{-1}
a	Constant relating wave power density to volumetric marsh loss	kPa^{-1}
$R_{(x,y,t)}$	Annual erosion rate at position (x,y) and time t	m yr^{-1}
$\overline{P}_{(x,y,t)}$	Average wave power density upon impact at (x,y) and time t	m yr^{-1}
$c_{(x,y)}$	Soil shear strength at position (x,y)	kPa
	Cellular automaton model formulation (equations (6) and (7))	
$p_{(x_i,y_i),\Delta t}$	Probability that the ith marsh element transitions from a marsh state to an open water state during time interval ranging from t to $t+\Delta t$	—
$R_{(x_i,y_i,t)}$	Predicted erosion rate of the ith marsh element as described by equation (4)	m yr^{-1}
n_t	Number of marsh elements that are part of the marsh edge at time t	—
Δt	Time interval during which there is a 100% probability of (at least) one marsh element eroding	year
	Analytical approximation through scale transition theory (equation (8))	
$\overline{R}$	Average annual erosion of the shoreline over the marsh site	
$\overline{c}$	Average soil shear strength across the marsh site	kPa
σ_c	Standard deviation of soil shear strength for the marsh site	kPa
	Quantification of front roughness (equation (9))	
ω	Roughness of the eroding marsh front	m
L_y	The number of rows in the model lattice (perpendicular to the erosion direction)	—
$h_{(x_i,y_i)}$	Distance of the frontrunner (to a reference point) at the ith row of the model lattice	m
$\overline{h}_{(x,y)}$	The average distance of all frontrunners (to a reference point) in the model lattice	m

response of R to changes in $\overline{P}$ is strongly dependent on the value of c, allowing the potential for large within-site variation if a single marsh site captures some portion of the wide range of c values observed across sites (Marani et al., 2011). To consider the influence of variable soil shear strength on R, our simplification of equation (1) retains c and specifies its position within the marsh. Linearity between R and $\overline{P}$ has been observed within sites when constant h is assumed (Marani et al., 2011; Schwimmer, 2001), which supports using the following relation:

$$R_{(x,y,t)} = \frac{\varphi \overline{P}_{(x,y,t)}}{c_{(x,y)}} \tag{4}$$

where (x,y,t) indicates a position within the marsh at time t and $\varphi \equiv f(h/d)/h$ (in m^{-1}) is introduced to represent a site-specific constant that includes a unit conversion between the timescales of wave action (in s) and marsh erosion (in years).

For spatial scales on the order of a kilometer or less, it is reasonable to assume that the strength and direction of wave power density prior to impact, $\vec{P}$, are uniform (e.g., Leonardi & Fagherazzi, 2015). Because shoreline geometry varies, wave power density upon impact at location (x,y) will depend on $\alpha_{(x,y,t)}$, the angle of inbound waves relative to shore-normal at time t. Due to the dynamic nature of the marsh shoreline, exposure of marsh edges at location (x,y) changes over time as well, which results in the time-dependency of $\overline{P}_{(x,y,t)}$. The relationship can be described by

$$\overline{P}_{(x,y,t)} = \overline{|\vec{P}| \cos\alpha_{(x,y,t)}} \tag{5}$$

where vector $\vec{P}$ is wave power density prior to impact and $\alpha_{(x,y,t)}$ is the angle of $\vec{P}$ relative to shore-normal at position (x,y) at time t (Marani et al., 2011). Thus, introducing $c_{(x,y)}$ and $\overline{P}_{(x,y,t)}$ enables studying the effects of

local variation in erosion resistance (i.e., soil shear strength) and wave power density on local erosion rates $R_{(x,y,t)}$.

Equation (4) was implemented in a stochastic cellular automaton model, following the framework presented by Leonardi and Fagherazzi (2014, 2015). In this framework, space is discretized as a square-tiled lattice of 256 × 256 cells. Each cell represents one square meter that can be either in a marsh or open water state. Marsh cells composing the marsh edge (i.e., cells sharing at least one edge with open water) transition to water with probability (Leonardi & Fagherazzi, 2014, 2015):

$$p_{(x_i,y_i),\Delta t} = \frac{R_{(x_i,y_i,t)}}{\sum_{j=1}^{n_t} R_{(x_j,y_j)}} \tag{6}$$

where Δt is the time interval considered, $R_{(x_i,y_i,t)}$ is the predicted erosion rate of element i as described by equation (4), and n_t is the number of cells that are part of the marsh edge at time t. As noted by Leonardi and Fagherazzi (2014, 2015), numerical studies of etching processes in composite media (Kolwankar et al., 2003; Štěpánek, 2008; Xin, 2000) have shown that equations such as (6) can be implemented as event-based algorithms that use a dynamic Δt:

$$\Delta t = \frac{1}{\sum_{j=1}^{n_t} R_{(x_j,y_j)}} \tag{7}$$

At the end of a model iteration, cells or groups of cells surrounded by water on all sides automatically erode to mimic mass failure following Leonardi and Fagherazzi (2014, 2015). In contrast to prior simulation studies, we relaxed the assumption of unidirectionality of inbound wind and waves. Instead, natural variation in wind direction was incorporated by equally distributing the angle of inbound waves at time t over three sequential multiples of 45°, with an average $\vec{P}$ normal to the initial shoreline. Hence, a marsh cell was more likely to transition at a particular time step if more sides were exposed to open water. Simulations were run until 50% of the initial marsh had eroded (Leonardi & Fagherazzi, 2014, 2015).

2.2. Analyses

To assess the influence of spatial heterogeneity on marsh shoreline erosion, we first explored how the integrated theoretical framework related within-site spatial variation in erosion resistance to local variability in shoreline erosion. We parameterized φ using field measurements of $c_{(x,y)}$ and $R_{(x,y)}$ taken in 12 plots along a 1-km shoreline of a Louisiana salt marsh (29°26′40.8″N 89°53′28.7″W; Bernik, 2015; Blum et al., 2014; Zengel et al., 2015), and we used data on wind direction and speed from a proximate NOAA buoy station to calculate $\overline{P}$ (Figure S3; see Text S3 for details).

We then compared analytical approximations of long-term average marsh erosion rates with model simulations to assess how spatial heterogeneity and shoreline geometry mediate erosion. Application of scale transition theory (Melbourne & Chesson, 2006) to equation (4) yielded an analytical approximation of the average erosion rate of a spatially heterogeneous marsh:

$$\overline{R} = \frac{\varphi \overline{P}}{\overline{c}} + \sigma_c^2 \frac{\varphi \overline{P}}{\overline{c}^3} \tag{8}$$

in which the overbars indicate spatial averages and σ_c^2 is the variance of c (referred to as the magnitude of spatial heterogeneity from here forward, in kPa^2). We also assessed erosion with spatial heterogeneity organized in clonal patches (varying between 5 and 1,000 m^2 in separate simulations; see Text S4 for details), representing the clonal growth form of smooth cordgrass (Grace, 1993; Sosnová et al., 2010; Travis & Hester, 2005). Each simulation included 10 patch types that differed in soil shear strength, reflecting phenotypic variation in functional traits among clones as demonstrated in previous experiments (Figures S1 and S2; see Text S1 and S2 for details; Bernik, 2015). Simulations including clonal patches were compared to control simulations in which the same marsh cells (and associated $c_{(x,y)}$ values) were randomized in space. This randomization procedure effectively removed spatial structure from the simulated marshes, as the average clone size was reduced to nearly the minimum size of one cell, regardless of the average prerandomization clone size (average clone size after randomization: 1.2470 ± 0.0002 cells; Figure S4; see Text S4 for further details). Comparisons between the patchy marshes and control simulations were drawn for low and high spatial heterogeneity according to 30 replicates for each combination of clone size and spatial

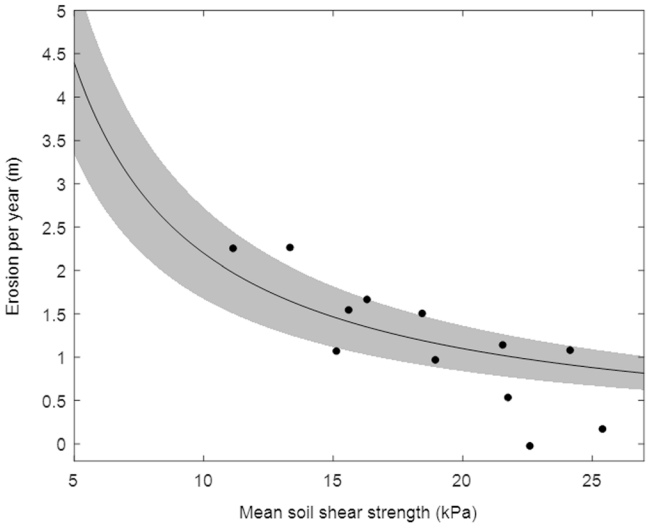

Figure 1. Erosion as a function of within-site variation in soil shear strength, showing field data from a marsh shoreline in Bay Jimmy (LA, USA; see Text S2 for details). Most observations fall within the shaded 95% confidence interval of values predicted by the analytical marsh erosion function, derived from Marani et al. (2011); (equation (4)). The solid line indicates the model fit, using the estimated parameter $\varphi\overline{P} = 22.01 \pm 5.23$.

heterogeneity. Simulations used an empirical estimate of mean wave power density, which did result in qualitative differences from simulations assuming either higher or lower mean wave power density (Figures S5–S7).

Finally, we assessed how the clonal patch structure of marshes affects spatiotemporal patterns of marsh shoreline erosion. Using the same range of patch sizes noted above and 30 replicate simulations of each, we assessed interannual variation in the extent of marsh erosion. We also assessed whether shoreline geometry reflects temporal variation in erosion. Shoreline geometry was quantified as the roughness of the marsh's eroding front at the end of each simulation. This metric is similar to the fractal dimension used by Leonardi, Defne, et al. (2016) but has also been used specifically for the study of front propagation (Eppinga et al., 2013; O'Malley et al., 2009). Front roughness was calculated as

$$\omega = \sqrt{\frac{1}{L_y}\sum_{i=1}^{L_y}\left(h_{(x_i,y_i)} - \overline{h_{(x,y)}}\right)^2} \tag{9}$$

in which ω is the front roughness (in m) and L_y is the number of rows in the lattice, which are ordered perpendicular to the main direction of erosion (dimensionless). Variable $h_{(x_i,y_i)}$ is the so-called frontrunner position (Eppinga et al., 2013; O'Malley et al., 2009) at the ith row of the marsh shoreline (in m). The average frontrunner position (in m) is $\overline{h_{(x,y)}}$. All simulations and statistical fitting procedures were performed in MATLAB (Mathworks, v. 2016a).

3. Results

3.1. Heterogeneity of Soil Shear Strength Predicts Within-Site Variation in Marsh Erosion

We found that equation (4) provided a highly significant fit with field measurements of longshore variation in soil shear strength and corresponding erosion rates ($R_{adj}^2 = 0.55$, $p = 1.7 \times 10^{-6}$), with the majority of observations falling within the 95% confidence interval of fitted model predictions (Figure 1).

3.2. Spatial Heterogeneity, Shoreline Morphology, and Patchiness Accelerate Erosion

In contrast to previous model simulations (Leonardi & Fagherazzi, 2014), application of scale transition theory analytically revealed that under our formulation (equations (4) and (8)), average rates of marsh shoreline erosion increase with increasing spatial heterogeneity in soil shear strength (Figure 2a). This effect was particularly strong for marshes characterized by low average soil shear strength (Figure 2a). This result highlights that the effect of spatial heterogeneity on marsh erosion depends on the nature of the relationship between soil shear strength and erosion probability. Comparison of analytical approximations (equation (8)) with cellular automaton simulations of eroding marshes (equations (6) and (7)) also indicates that the emergent morphology of erosional marsh shorelines, being exposed to wave power under varying wind directions, further increases erosion (Figures 2a and S8; see Text S5 for details). The strength of this effect was stronger when average soil shear strength was low (Figure 2a). When spatial variation was organized in clonal patches, marshes exhibited higher erosion rates than randomized control simulations (Figure 2b). This departure was more pronounced with higher spatial heterogeneity (Figure 2b). Differences in erosion rates peaked when patches were of intermediate size (of 20–200 m^2; Figure 2b). This result corresponded to above-average erosion events increasing in magnitude but decreasing in frequency as clone size increased (Figure S9).

3.3. Clonal Patch Size Controls Temporal Variability in Erosion and Increases Shoreline Roughness

Average patch size not only influenced the temporal pattern of shoreline erosion, it also influenced shoreline morphology (Figure 3). When the magnitude of average wave power and level of spatial heterogeneity in soil shear strength were kept constant, shoreline roughness increased with the size of clonal patches (Figures 3a and 3b). Increasing patch size also increased interannual variability in erosion (Figures 3b and 3c). Although

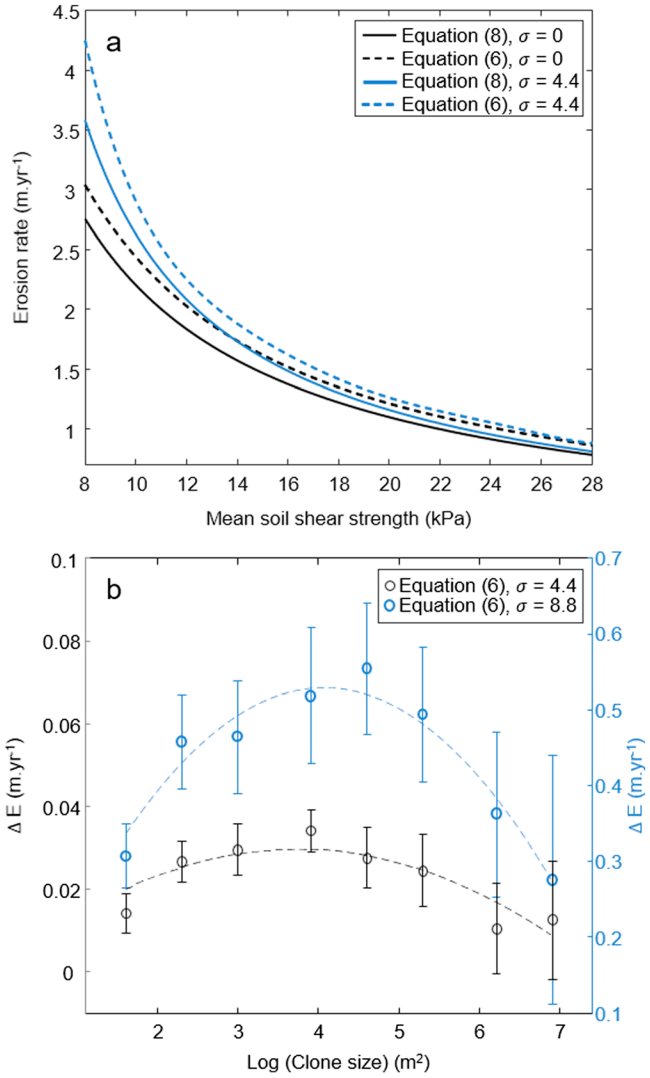

Figure 2. Effects of spatial variation on average rates of shoreline erosion. (a) Predictions for uniform marshes (solid black line) underestimate erosion, as shoreline morphology (dashed lines) and spatial heterogeneity within marshes (blue lines) accelerate erosion rates. In marshes characterized by high soil shear strength, shoreline morphology (black dashed line) forms the strongest driver of accelerated erosion, but spatial heterogeneity becomes more important as average soil shear strength decreases. The dashed lines represent higher order polynomial fits on erosion rates for 11 mean soil shear strength values, averaged over 30 replicate simulations; $R_{adj}^2 > 0.99$ for both fits. (b) The difference in erosion rates when heterogeneous soil shear strength is organized into clonal patches versus being randomly distributed (ΔE), showing that clonal organization accelerates erosion. The effect is elevated with greater spatial heterogeneity, and the effect is strongest when clones are of intermediate size (20–200 m^2). The dashed lines represent quadratic fits on erosion rates, averaged over 30 replicate simulations; σ = 4.4: $R_{adj}^2 = 0.76$; σ = 8.8: $R_{adj}^2 = 0.93$.

average erosion rates were relatively low for marshes with large patches (Figures 2b, S6, and S10), erosion in these marshes was characterized by the occurrence of prolonged periods of little erosion punctuated by large but rare erosion events (Figure S9). This temporal pattern suggests that erosion may be difficult to predict by extrapolating from short-term measurements. It is thus noteworthy that shoreline roughness may serve as a diagnostic feature of interannual variability in marsh erosion when this information is integrated with either the size distribution of clonal patches (Figures 3b and S11) or the spatial heterogeneity in soil shear stress created by clonal patches (Figure 3c).

4. Discussion and Conclusions

We found that well-established biogeomorphic interactions produce emergent effects on ecosystem-scale erosion dynamics. While previous studies have considered how wave power and randomly distributed spatial heterogeneity can drive variation in erosion rates and shoreline roughness (Leonardi & Fagherazzi, 2014, 2015; Marani et al., 2011), our results indicate that the size and diversity of plant clones constitute biological drivers of shoreline erosion and morphology. This highlights that ecological control over the physical process of marsh shoreline erosion is not simply a result of plant presence, or even community composition, but how plant populations and phenotypic variation are structured. Results from our model demonstrated that the relationship between soil shear strength and marsh erosion across sites holds for plot-scale measures taken along a single heterogeneous marsh shoreline (Figure 1). The nonlinear relationship between soil shear strength and erosion rate enables easily erodible sites to disproportionately contribute to marsh loss rates. This disproportionality is overlooked when predicting erosion rates based on spatially averaged soil shear strength (equation (8); Figure 2a). The magnitude of underestimation increases with decreasing soil shear strength or increasing spatial heterogeneity (equation (8); Figure 2a), which illustrates the importance of characterizing mean and variation in soil shear strength along a marsh shoreline.

Intriguingly, we found an interaction between the magnitude and organization of spatial heterogeneity (Figure 2b). The positive effect of soil heterogeneity on erosion rates can depend on its spatial patchiness, reflecting clonal patterns in landform engineers. Our results show that intermediately sized clones (20–200 m^2) exert the largest effect, increasing erosion by more than 10% compared to marshes with randomly distributed heterogeneity (Figure S10).

Integrating the relationship between soil shear strength and marsh erosion as proposed by Marani et al. (2011) into the simulation framework developed by Leonardi and Fagherazzi (2014, 2015) yielded qualitatively different outcomes from prior studies. Leonardi and Fagherazzi (2014) found that increasing spatial heterogeneity reduces average erosion rates, whereas we found that it increased erosion rates up to 30% for soil strengths observed in our field site (Figures 1 and 2a). This discrepancy derives from using different erosion functions than Leonardi and Fagherazzi (2014, 2015), who characterize the effect of soil variability as decreasing with increasing wave power (i.e., erosion becomes uniform as wave power increases relative to soil integrity). Differences in field estimates of soil shear strength may justify the use of alternate erosion models, as the Atlantic coast marshes evaluated by Leonardi and Fagherazzi (2015) exhibited much lower surface soil shear strength (1–4.5 kPa) compared to the Gulf coast marsh examined in

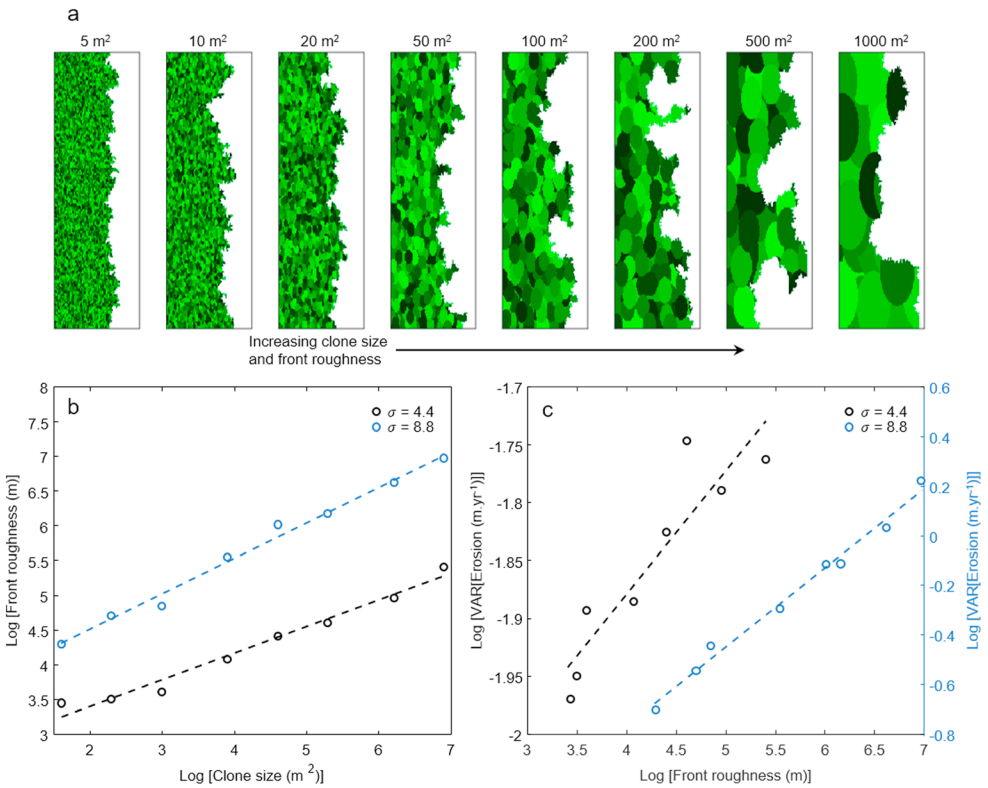

Figure 3. Effects of clonal organization on spatiotemporal patterns of shoreline erosion. (a) As clones increase in size, shoreline roughness increases (showing 50% of the initial marsh eroded). The colors indicate variation in soil shear strength induced by clonal patches. (b) Shoreline roughness increases monotonically with clonal patch size. The symbols indicate averages of 30 replicate simulations. The dashed lines indicate linear fits between log-transformed clone size and front roughness (low heterogeneity, $\sigma = 4.4$: $R_{adj}^2 = 0.97$, $p = 5.1 \times 10^{-6}$; high heterogeneity, $\sigma = 8.8$: $R_{adj}^2 = 0.98$, $p = 3.9 \times 10^{-7}$). (c) Increasing front roughness correlates with increasing interannual variation in erosion. The dashed lines indicate linear fits between log-transformed front roughness and interannual erosion variability (low heterogeneity, $\sigma = 4.4$: $R_{adj}^2 = 0.81$, $p = 0.0015$; high heterogeneity, $\sigma = 8.8$: $R_{adj}^2 = 0.99$, $p = 6.5 \times 10^{-7}$).

this study (Figure 1). Location dependence across models thereby hinges on whether soil shear strength is comparable to erosive forces, implying that shallow or weakly rooted sites, as in brackish marshes or recently disturbed areas, may exhibit reduced erosion in response to random spatial heterogeneity.

For typical high-productivity salt marshes dominated by species like *S. alterniflora*, wave power is unlikely to achieve a magnitude where uniform erosion becomes possible. For example, the extreme wave power observed during Hurricane Katrina generated enough wave shear stress to induce failure for strengths of up to 1.8 kPa (Howes et al., 2010), which is only a fraction of the soil strength recorded in Gulf coast salt marshes, yet salt marshes nonetheless experienced widespread erosion. This suggests that Gulf coast erosion results from progressive failure under the repeated and cumulative forcing of waves, as soil instability and root mat degradation increase in inverse proportion to soil strength (Bendoni et al., 2014; Francalanci et al., 2013; Leonardi, Ganju, et al., 2016), which is captured by the function proposed by Marani et al. (2011). For conditions where soil shear strength can similarly buffer erosion, our model suggests random spatial heterogeneity increases rates of erosion.

It is becoming increasingly evident that roughness can serve as a diagnostic feature for comparative assessments of erosion across marshes (Leonardi, Defne, et al., 2016; Priestas et al., 2015). Our results are consistent with previous work suggesting that shoreline roughness reflects temporal variability in erosion rates (Figure 3c), but we found a slightly different relationship driven by an alternative mechanism. Previous work attributed temporal variability to reduced wind wave forcing, whereas we found that it can be explained by increases in either spatial heterogeneity or clone size (Figure 3). This suggests that shorelines occupied by larger clones may require longer relative timeframes to accurately characterize average erosion rates.

Moreover, our results suggest that direct correlations between roughness and interannual variability are not sufficient, as a given roughness can consist of larger, more similar clones with low interannual variability or smaller, more differentiated clones with high interannual variability (Figures 3b and 3c). This problem can be circumvented by relating shoreline roughness to either spatial heterogeneity or the clonal patch size distribution, which is likely related to the age and disturbance history of a site (e.g., Bernik et al., 2016; Richards et al., 2004; Travis & Hester, 2005; for examples, see Figure S11). These findings help clarify and advance the theoretical framework for utilizing "snapshot" data measured at single points in time to infer long-term erosion dynamics.

Greater understanding of biogeomorphic systems could help mitigate land loss by informing coastal restoration and protection (Corenblit et al., 2007, 2011; Larsen et al., 2014, 2016). So far, restoration and management plans—including the $50B Louisiana Coastal Master Plan, which sets forth a path to sustain the largest coastal wetlands complex in North America (Louisiana Coastal Protection and Restoration Authority, 2017)—have not accounted for the possibility that biologically determined spatial organization may govern erosion dynamics. Filling this knowledge gap by further discerning the nature and relative importance of biogeomorphic drivers of marsh shoreline erosion could guide prioritization and investments. Our approach illustrates the usefulness of reduced complexity models to explore questions that fall at disciplinary interfaces and the need for similar investigations to help advance understanding of biogeomorphic systems over ecological and evolutionary time scales (Corenblit et al., 2007, 2011; Kolker et al., 2010; Larsen et al., 2014, 2016).

Acknowledgments
The authors thank J. Karubian, D.R. Strong, and C.M. Taylor for comments that improved the manuscript. This work was supported by an EPA STAR Fellowship awarded to B.M.B. Wind data were obtained freely from the National Data Buoy Center (http://www.ndbc.noaa.gov/). Model code and input data are included as supporting information.

References

Bendoni, M., Francalanci, S., Cappietti, L., & Solari, L. (2014). On salt marshes retreat: Experiments and modeling toppling failures induced by wind waves. *Journal of Geophysical Research: Earth Surface*, *119*, 603–620. https://doi.org/10.1002/2013JF002967

Bernik, B. M. (2015). Ecosystem consequences of genetic variation in the salt marsh engineer Spartina alterniflora (PhD thesis), New Orleans, LA: Dep. of Ecol. and Evolutionary Biology, Tulane Univ.

Bernik, B. M., Li, H., & Blum, M. J. (2016). Genetic variation of Spartina alterniflora intentionally introduced to China. *Biological Invasions*, *18*(5), 1485–1498. https://doi.org/10.1007/s10530-016-1096-3

Blum, M. J., Bernik, B. M., Azwell, T., & Hoek, E. M. V. (2014). Remediation and restoration of northern Gulf of Mexico coastal ecosystems following the Deepwater Horizon event. In P. Somasundaran, et al. (Eds.), *Oil spill remediation*, (pp. 59–88). Hoboken, NJ: John Wiley. https://doi.org/10.1002/9781118825662.ch3

Corenblit, D., Baas, A. C. W., Bornette, G., Darrozes, J., Delmotte, S., Francis, R. A., et al. (2011). Feedbacks between geomorphology and biota controlling Earth surface processes and landforms: A review of foundation concepts and current understandings. *Earth-Science Reviews*, *106*(3–4), 307–331. https://doi.org/10.1016/j.earscirev.2011.03.002

Corenblit, D., Tabacchi, E., Steiger, J., & Gurnell, A. M. (2007). Reciprocal interactions and adjustments between fluvial landforms and vegetation dynamics in river corridors: A review of complementary approaches. *Earth-Science Reviews*, *84*(1–2), 56–86. https://doi.org/10.1016/j.earscirev.2007.05.004

Eppinga, M. B., Pucko, C. A., Baudena, M., Beckage, B., & Molofsky, J. (2013). A new method to infer vegetation boundary movement from "snapshot" data. *Ecography*, *36*(5), 622–635. https://doi.org/10.1111/j.1600-0587.2012.07753.x

Fagherazzi, S., Kirwan, M. L., Mudd, S. M., Guntenspergen, G. R., Temmerman, S., D'Alpaos, A., et al. (2012). Numerical models of salt marsh evolution: Ecological, geomorphic, and climatic factors. *Reviews of Geophysics*, *50*, RG1002. https://doi.org/10.1029/2011RG000359

Fagherazzi, S., Mariotti, G., Wiberg, P., & McGlathery, K. (2013). Marsh collapse does not require sea level rise. *Oceanography*, *26*(3), 70–77. https://doi.org/10.5670/oceanog.2013.47

Francalanci, S., Bendoni, M., Rinaldi, M., & Solari, L. (2013). Ecomorphodynamic evolution of salt marshes: Experimental observations of bank retreat processes. *Geomorphology*, *195*, 53–65. https://doi.org/10.1016/j.geomorph.2013.04.026

Grace, J. B. (1993). The adaptive significance of clonal reproduction in angiosperms: An aquatic perspective. *Aquatic Botany*, *44*(2-3), 159–180. https://doi.org/10.1016/0304-3770(93)90070-D

Howes, N. C., FitzGerald, D. M., Hughes, Z. J., Georgiou, I. Y., Kulp, M. A., Miner, M. D., et al. (2010). Hurricane-induced failure of low salinity wetlands. *Proceedings of the National Academy of Sciences of the United States of America*, *107*(32), 14,014–14,019. https://doi.org/10.1073/pnas.0914582107

Kirwan, M., & Temmerman, S. (2009). Coastal marsh response to historical and future sea-level acceleration. *Quaternary Science Reviews*, *28*(17–18), 1801–1808. https://doi.org/10.1016/j.quascirev.2009.02.022

Kolker, A. S., Allison, M. A., & Hameed, S. (2011). An evaluation of subsidence and sea-level variability in the northern Gulf of Mexico. *Geophysical Research Letters*, *38*, L21404. https://doi.org/10.1029/2011GL049458

Kolker, A. S., Kirwan, M. L., Goodbred, S. L., & Cochran, J. K. (2010). Global climate changes recorded in coastal wetland sediments: Empirical observations linked to theoretical predictions. *Geophysical Research Letters*, *37*, L14706. https://doi.org/10.1029/2010GL043874

Kolwankar, K. M., Plapp, M., & Sapoval, B. (2003). Percolation-dependent reaction time in the etching of disordered solids. *Europhysics Letters*, *62*(4), 519–525. https://doi.org/10.1209/epl/i2003-00382-3

Larsen, L. G., Eppinga, M. B., Passalacqua, P., Getz, W. M., Rose, K. A., & Liang, M. (2016). Appropriate complexity landscape modeling. *Earth Science Reviews*, *160*, 111–130. https://doi.org/10.1016/j.earscirev.2016.06.016

Larsen, L. G., Thomas, C., Eppinga, M. B., & Coulthard, T. (2014). Exploratory modelling: Extracting causality from complexity. *Eos*, *95*(32), 285–286. https://doi.org/10.1002/2014EO320001

Leonardi, N., Defne, Z., Ganju, N. K., & Fagherazzi, S. (2016). Salt marsh erosion rates and boundary features in a shallow bay. *Journal of Geophysical Research: Earth Surface*, *121*, 1861–1875. https://doi.org/10.1002/2016JF003975

Leonardi, N., & Fagherazzi, S. (2014). How waves shape salt marshes. *Geology*, *42*(10), 887–890. https://doi.org/10.1130/G35751.1

Leonardi, N., & Fagherazzi, S. (2015). Effect of local variability in erosional resistance on large-scale morphodynamic response of salt marshes to wind waves and extreme events. *Geophysical Research Letters*, *42*, 5872–5879. https://doi.org/10.1002/2015GL064730

Leonardi, N., Ganju, N. K., & Fagherazzi, S. (2016). A linear relationship between wave power and erosion determines salt-marsh resilience to violent storms and hurricanes. *Proceedings of the National Academy of Sciences of the United States of America*, *113*(1), 64–68. https://doi.org/10.1073/pnas.1510095112

Louisiana Coastal Protection and Restoration Authority (2017). *Louisiana's comprehensive master plan for a sustainable coast* (pp. 167). Baton Rouge, Louisiana: Coastal Protection and Restoration Authority. Retrieved from http://coastal.la.gov/our-plan/2017-coastal-master-plan

Marani, M., D'Alpaos, A., Lanzoni, S., & Santalucia, M. (2011). Understanding and predicting wave erosion of marsh edges. *Geophysical Research Letters*, *38*, L21401. https://doi.org/10.1029/2011GL048995

Mariotti, G., & Fagherazzi, S. (2010). A numerical model for the coupled long-term evolution of salt marshes and tidal flats. *Journal of Geophysical Research*, *115*, F01004. https://doi.org/10.1029/2009JF001326

McLoughlin, S. M., Wiberg, P. L., Safak, I., & McGlathery, K. J. (2015). Rates and forcing of marsh edge erosion in a shallow Coastal Bay. *Estuaries and Coasts*, *38*(2), 620–638. https://doi.org/10.1007/s12237-014-9841-2

Melbourne, B. A., & Chesson, P. (2006). The scale transition: Scaling up population dynamics with field data. *Ecology*, *87*(6), 1478–1488. https://doi.org/10.1890/0012-9658(2006)87[1478:TSTSUP]2.0.CO;2

Michel, J., Owens, E. H., Zengel, S., Graham, A., Nixon, Z., Allard, T., et al. (2013). Extent and degree of shoreline oiling: Deepwater Horizon oil spill, Gulf of Mexico, USA. *PLoS One*, *8*(6), e65087. https://doi.org/10.1371/journal.pone.0065087

Millennium Ecosystem Assessment (2005). *Ecosystems and human well-being—Synthesis report*. Washington, DC: World Resources Institute.

Möller, I., Kudella, M., Rupprecht, F., Spencer, T., Paul, M., van Wesenbeeck, B. K., et al. (2014). Wave attenuation over coastal salt marshes under storm surge conditions. *Nature Geoscience*, *7*(10), 727–731. https://doi.org/10.1038/ngeo2251

O'Malley, L., Korniss, G., & Caraco, T. (2009). Ecological invasion, roughened fronts, and a competitor's extreme advance: integrating stochastic spatial-growth models. *Bulletin of Mathematical Biology*, *71*(5), 1160–1188. https://doi.org/10.1007/s11538-009-9398-6

Priestas, A. M., Mariotti, G., Leonardi, N., & Fagherazzi, S. (2015). Coupled wave energy and erosion dynamics along a salt marsh boundary, Hog Island Bay, Virginia, USA. *Journal of Marine Science and Engineering*, *3*(3), 1041–1065. https://doi:10.3390/jmse3031041

Richards, C. L., Hamrick, J. L., Donovan, L. A., & Mauricio, R. (2004). Unexpectedly high clonal diversity of two salt marsh perennials across a severe environmental gradient. *Ecology Letters*, *7*(12), 1155–1162. https://doi.org/10.1111/j.1461-0248.2004.00674.x

Schwimmer, R. A. (2001). Rates and processes of marsh shoreline erosion in Rehoboth Bay, Delaware, USA. *Journal of Coastal Research*, *17*(3), 672–683. Retrieve from http://www.jstor.org/stable/4300218

Sosnová, M., van Diggelen, R., & Klimešová, J. (2010). Distribution of clonal growth forms in wetlands. *Aquatic Botany*, *92*(1), 33–39. https://doi.org/10.1016/j.aquabot.2009.09.005

Štěpánek, F. (2008). Effect of microstructure and pure component properties on the dissolution rate of a binary composite material. *Computational Materials Science*, *44*(1), 145–151. https://doi.org/10.1016/j.commatsci.2008.01.037

Travis, S. E., & Hester, M. W. (2005). A space-for-time substitution reveals the long-term decline in genotypic diversity of a widespread salt marsh plant, Spartina alterniflora, over a span of 1500 years. *Journal of Ecology*, *93*(2), 417–430. https://doi.org/10.1111/j.0022-0477.2005.00985.x

Turner, R. (2011). Beneath the salt marsh canopy: Loss of soil strength with increasing nutrient loads. *Estuaries and Coasts*, *34*(5), 1084–1093. https://doi.org/10.1007/s12237-010-9341-y

van Eerdt, M. M. (1985). The influence of vegetation on erosion and accretion in salt marshes of the Oosterschelde, the Netherlands. *Vegetatio*, *62*(1–3), 367–373. https://doi.org/10.1007/BF00044763

Wilson, C. A., & Allison, M. A. (2008). An equilibrium profile model for retreating marsh shorelines in southeast Louisiana. *Estuarine, Coastal and Shelf Science*, *80*(4), 483–494. https://doi.org/10.1016/j.ecss.2008.09.004

Wilson, C. A., Hughes, Z. J., & FitzGerald, D. M. (2012). The effects of crab bioturbation on mid-Atlantic salt marsh tidal creek extension: Geotechnical and geochemical changes. *Estuarine, Coastal and Shelf Science*, *106*, 33–44. https://doi.org/10.1016/j.ecss.2012.04.019

Xin, J. (2000). Front propagation in heterogeneous media. *SIAM Review*, *42*(2), 161–230. https://doi.org/10.1137/S0036144599364296

Zengel, S., Bernik, B. M., Rutherford, N., Nixon, Z., & Michel, J. (2015). Heavily oiled salt marsh following the Deepwater Horizon oil spill, ecological comparisons of shoreline cleanup treatments and recovery. *PLoS One*, *10*(7), e0132324. https://doi.org/10.1371/journal.pone.0132324

Zengel, S., & Michel, J. (2013). Deepwater Horizon oil spill: Salt marsh oiling conditions, treatment testing, and treatment history in northern Barataria Bay, Louisiana (Interim Report October 2011). U.S. Department of Commerce, NOAA Techn. Memorandum NOS OR&R 42. Seattle, WA: Emergency Response Division, NOAA, pp. 74. Retrieve from http://response.restoration.noaa.gov/deepwater_horizon